



This is a repository copy of *Computing backbone curves for nonlinear oscillators with higher order polynomial stiffness terms*.

White Rose Research Online URL for this paper:  
<http://eprints.whiterose.ac.uk/170958/>

Version: Accepted Version

---

**Proceedings Paper:**

Nasir, A.M., Sims, N.D. and Wagg, D.J. [orcid.org/0000-0002-7266-2105](https://orcid.org/0000-0002-7266-2105) (2020) Computing backbone curves for nonlinear oscillators with higher order polynomial stiffness terms. In: Papadrakakis, M., Fragiadakis, M. and Papadimitriou, C., (eds.) EURODYN 2020: Proceedings of the XI International Conference on Structural Dynamics. EURODYN 2020: XI International Conference on Structural Dynamics, 23-26 Nov 2020, Athens, Greece. European Association for Structural Dynamics (EASD) , pp. 318-334. ISBN 9786188507203

10.47964/1120.9026.19584

---

© 2020 The Authors. This is an author-produced version of a paper subsequently published in EURODYN 2020 Proceedings.

**Reuse**

Items deposited in White Rose Research Online are protected by copyright, with all rights reserved unless indicated otherwise. They may be downloaded and/or printed for private study, or other acts as permitted by national copyright laws. The publisher or other rights holders may allow further reproduction and re-use of the full text version. This is indicated by the licence information on the White Rose Research Online record for the item.

**Takedown**

If you consider content in White Rose Research Online to be in breach of UK law, please notify us by emailing [eprints@whiterose.ac.uk](mailto:eprints@whiterose.ac.uk) including the URL of the record and the reason for the withdrawal request.



[eprints@whiterose.ac.uk](mailto:eprints@whiterose.ac.uk)  
<https://eprints.whiterose.ac.uk/>

## COMPUTING BACKBONE CURVES FOR NONLINEAR OSCILLATORS WITH HIGHER ORDER POLYNOMIAL STIFFNESS TERMS

Ayman M. Nasir<sup>1</sup>, Neil D. Sims<sup>2</sup>, David J. Wagg<sup>2</sup>

<sup>1</sup> PhD Student – University of Sheffield  
Sheffield, S1 3JD, UK  
e-mail: amnasir1@sheffield.ac.uk

<sup>2</sup> Prof. in Mechanical Engineering Dep. - University of Sheffield  
Sheffield, S1 3JD, UK  
e-mail: n.sims@sheffield.ac.uk, david.wagg@sheffield.ac.uk

**Keywords:** Nonlinear, Vibrations, Normal forms, Backbone curves, Symbolic computations.

**Abstract.** *Single-degree-of-freedom (SDOF) nonlinear oscillators are widely used for modeling systems with just one degree-of-freedom in addition to single mode approximations to structural elements such as beams and cables, as well as other multi-degree-of-freedom (MDOF) applications. In this work, an investigation of the behavior of SDOF nonlinear oscillators is carried out using the method of direct normal forms. So far, this method has only been considered as a theoretical technique used for solving limited nonlinear dynamical systems in which low orders of nonlinearities appear, involving quadratic and cubic nonlinearities. In this work, thanks to the implementation of symbolic computations, the method of direct normal forms is generalized for solving nonlinear SDOF systems with any order of polynomial (or geometric) weak nonlinearities. Using this new approach, the effect of any higher order nonlinear term, or any combination of nonlinear terms can be investigated. Backbone curve relations are obtained for a selection of example systems representing both hardening and softening systems, and the results are verified by comparing the approximate analytical solutions to numerical solutions generated using COCO numerical continuation toolbox in Matlab.*

## 1 INTRODUCTION

Nonlinear normal forms method is a well-established technique for obtaining approximate solutions for nonlinear oscillators with various types of weak (typically smooth) nonlinearities. In principle, it can be used for either SDOF or MDOF problems; although for systems with more than a few degrees-of-freedom the algebraic complexity quickly escalates. It is also possible for the analyst to select certain resonant (or non-resonant) cases to study, by making one (or sometimes more) near-identity transforms [3]. The analytical basis of the technique is to use matrix algebra via a series of analytical steps that finally detect the desired resonances and can be used to find approximate solutions, such as so-called backbone curves, for the SDOF or MDOF system being considered.

While this method has the potential to be applied for a wide range of applications, it can generate large and complicated mathematical terms. As a result, it could be helpful to use symbolic packages, which can deal with such complex mathematical expressions and also offer the possibility of enhancing the accuracy of solution by increasing the number of terms truncated in the solution.

Another way to simplify such computations is to reduce the system order prior to computation. This is a pragmatic way to decrease the matrix sizes involved, however the size of the residual terms (i.e. those excluded by the reduction) should be estimated in order to ensure the accuracy of the final solution. Using a computation package, such as Maple software, makes it possible to build a highly structured code that can, in principle, solve for any order of nonlinearity and potentially a large number of nonlinear terms. In this work, the number of terms is limited to two.

The origin of the idea of normal form transformations is attributed to the work of Poincaré. Following this, the application of normal forms method for SDOF and MDOF is discussed widely in the literature. Notably the Hamiltonian normal form (and Birkhoff normal forms) were introduced for conservative dynamical systems [21], and are typically used to model undamped unforced applications in physics and engineering. The work of Arnold [22] did much to extend and promote the idea of normal form transformation in engineering mechanics. The normal form approach was extended to problems of forced and damped systems of coupled nonlinear oscillators by Jezequel and Lamarque, [24], and given recast in a perturbation framework by Nayfeh [25].

Because most mechanical vibration problems are naturally described by sets of second-order differential equations, a variant of the normal forms method applied directly to second order dynamical problems was first introduced by Neild and Wagg in [3]. The authors originally referred to this modified technique as ‘second order normal forms’. This approach will be used during the formulation and discussion in this work.

Compared with other techniques, the primary advantage of the direct normal forms is the ability of inherently computing the harmonics without pre-assuming any specific harmonic components included in trial solutions. Thus, no prior knowledge of the harmonic components in the response of the system is required and no additional complexity is needed when considering the harmonics. Furthermore, the process of direct normal forms can be formulated in a matrix-based manner, which makes its application more appropriate for the computer automation.

The direct normal form technique has been used in a number of conducted research works, investigating nonlinear dynamics of mechanical systems. Xin et al., [9], considered the SDOF nonlinear oscillators of polynomial-type nonlinearities using the direct normal form technique, their work involved investigation of velocities and displacements, whilst illustrating the contributions of the different polynomial nonlinearities in different forms to the system response by the resulting resonance response functions (RRFs).

Shaw et al. [23], studied the performance of the nonlinear vibration isolator using the direct normal form technique. The system was modelled as a SDOF oscillator with cubic and quintic nonlinear terms. The authors estimated a group of backbone curves of the nonlinear vibration isolator by considering its equivalent conservative system. Cammarano et al. [9] investigated the optimal load for the nonlinear energy harvester in the case of purely resistive loads. Their work was carried out both analytically and numerically, and the results showed that analytical solutions obtained using direct normal forms were in very close agreement with the numerical results within the frequency range of interest. The direct normal form technique was also applied to study the nonlinear dynamic behaviors of MDOF systems, see for example [9] and references therein.

However, in order to generalise the applications of direct normal forms, thanks to the implementation of Maple symbolic computations, this work focuses on studying SDOF nonlinear systems with higher orders of geometric nonlinearities. One reason for taking this approach is that, when attempting the direct normal forms analysis of such systems, usual hand calculations, can be extremely difficult as the number of terms included increases.

Due to the inherent nature of nonlinearities, the use of direct normal forms is not limited to nonlinear oscillators; many real-life engineering applications exhibit geometric, or even damping nonlinearities quite naturally. Therefore, the direct normal form technique has been used to study nonlinear beams, cables, shells, plates and multi-storey buildings - see [3] for detailed description of many of these applications. In this work, the direct normal forms method is used to analyse some SDOF oscillators with one, or two, geometric nonlinear terms. The application of this method, with the aid of symbolic computation algorithm, enables a robust computational method for the investigation of the dynamics exhibited by these types of oscillators using backbone curves.

## 2 DIRECT NORMAL FORMS METHODOLOGY

For the case of unforced vibrating systems, the technique is applied using four main consecutive steps:

- Step 1: Linear modal transformation in order to decouple the linear terms.
- Step 2: Derivation of the equation of motion for the nonlinear transformation.
- Step 3: Applying the near-identity transform.
- Step 4: Solving the resulting normal forms equation (or equations).

In addition, studying systems that are externally forced usually requires one further transformation, in which, any non-resonant forcing terms are to be excluded. Finally, damping term (usually viscous damping) is normally included within the nonlinear vector.

### 2.1 Computation of backbone curves using direct normal forms

Consider the case of nonlinear forced-damped SDOF oscillator, whose equation of motion may be written as

$$M \ddot{x}(t) + C \dot{x}(t) + K x(t) + N_x(x, \dot{x}, r) = P_x \mathbf{r}, \quad (1)$$

where the over dots represent derivation with respect to time,  $x$  represents the physical displacements,  $M$ ,  $C$  and  $K$  denote the mass, damping coefficient and linear stiffness respectively,  $N_x(x)$  is the nonlinear restoring force,  $\varepsilon$  is used to denote smallness of the nonlinear terms, the amplitude of the forcing term is denoted by  $P_x$ , and  $\mathbf{r}$  is the forcing vector which can be written as  $\mathbf{r} = \{r_p, r_m\}^T = \{e^{i\Omega t}, e^{-i\Omega t}\}^T$  where the forcing frequency is denoted by  $\Omega$ .

As mentioned earlier, direct normal forms analysis is applied using four main steps, for convenience, only key parts of the analysis are to be discussed in this work while the complete detailed analysis of this type of systems is extensively discussed in [3]. Moreover, for the application of the direct normal form technique, the nonlinear terms are assumed to be expressed in a polynomial form in terms of  $x$ .

From Eq. (1) all nonlinear terms are gathered in one term,  $\bar{N}_x(x)$ . Herein, both damping and nonlinear terms are assumed to be efficiently small compared to the linear stiffness and the forcing term, hence, more conveniently Eq. (2) can be rewritten as

$$M \ddot{x}(t) + K x(t) + \bar{N}_x(x, \dot{x}, r) = P_x \mathbf{r}, \quad (2)$$

where  $\bar{N}_x(x, \dot{x}, r) = N_x(x, \dot{x}, r) + C \dot{x}(t)$

Now, the application of direct normal forms begins, by writing Eq. (2) in its *linear modal normal form*, using the transformation  $x \rightarrow q$ , simply by applying  $x = \Phi q$ , where  $\Phi$  is the matrix containing the mode shapes, then, Eq. (2) becomes

$$\ddot{q} + \Lambda q + \bar{N}_q(q, \dot{q}, \mathbf{r}) = \mathbf{P}_q \mathbf{r}, \quad (3)$$

$$\text{where } \bar{N}_q(q, \dot{q}, \mathbf{r}) = (\Phi^T M \Phi)^{-1} \Phi^T \bar{N}_x(\Phi q, \Phi \dot{q}, \mathbf{r}), \quad \mathbf{P}_q = (\Phi^T M \Phi)^{-1} \Phi^T \mathbf{P}_x$$

Herein,  $q = u + \varepsilon H(u)$  where  $u$  and  $H(u)$  are the fundamental and harmonic components of  $q$  respectively.

The assumed solution has the form

$$u = u_p + u_m = \left( \frac{U}{2} e^{-i\phi} \right) e^{i\omega_n t} + \left( \frac{U}{2} e^{i\phi} \right) e^{-i\omega_n t}, \quad (4)$$

Where  $U$ ,  $\phi$  and  $\omega_n$  are the displacement amplitude, phase lag, and response frequency, respectively.

In order to complete the analysis,  $\bar{N}_q$ , in view of Eq. (4), should be decomposed into two vector  $\mathbf{n}^*$  and  $\mathbf{u}^*$  where  $\mathbf{n}^*$  is a row vector contains the coefficients part and  $\mathbf{u}^*$  is a column vector represents the nonlinear functions of  $u$ .

For the case of polynomial nonlinear terms (as appears in Eq. 2), the  $\ell^{\text{th}}$  element of  $\mathbf{u}^*$  may be written as

$$u_\ell^* = u_{pn}^{s_{p,\ell}} u_{mn}^{s_{m,\ell}} \quad (5)$$

Where  $s_{p,\ell}$  and  $s_{m,\ell}$  are exponents of  $u_p$  and  $u_m$  in the  $\ell^{\text{th}}$  element of  $\mathbf{u}_{(j)}^*$  respectively. This step is symbolically done in the proposed algorithm for every term in  $\mathbf{u}^*$ . In order to identify the resonant nonlinear terms retained in  $\mathbf{n}_{u(j)}$  from  $\mathbf{n}_{(j)}$ , a vector  $\beta_{(j)}$ , is introduced, i.e.

$$\beta_{(j)n,\ell} = \left[ \sum_{n=1}^N (s_{pj,\ell,n} - s_{mj,\ell,n}) \omega_m \right]^2 - \omega_m^2 \quad (6)$$

Finding  $\beta^*$  matrix is crucially important to complete the analysis, and it is performed symbolically with a series of iterative loops that capture the power indices in Eq. (5) and then substitute the result in Eq. (6).

The procedure discussed above is a short summary of the direct normal forms technique. In the following subsection, two examples of SDOF nonlinear oscillators are studied; the first example represents a SDOF conservative (unforced and undamped) oscillator with two different orders of geometric nonlinearities, whereas the second example is a SDOF oscillator with

viscous damping and harmonic forcing applied away from resonance. Lastly, the frequency response of a general system of a forced damped nonlinear oscillator with two types of geometric nonlinearities is studied. It is important to mention that all manipulations and solutions to be shown are computed using Maple symbolic computation packages with the aid of the COCO toolbox in Matlab for numerical comparisons and verifications.

## 2.2 SDOF conservative oscillator with various nonlinearities

Considering the following general formula for unforced, un-damped SDOF oscillator,

$$\ddot{x}(t) + \omega_n^2 x(t) + \alpha_1 x^\mu(t) + \alpha_2 x^\nu(t) = 0, \quad (7)$$

where  $\omega_n$  is the natural frequency of the system,  $\alpha_1$  and  $\alpha_2$  are arbitrary small coefficients for the nonlinear terms,  $\mu$  and  $\nu$  are the lower and higher orders of the nonlinear terms, respectively. Furthermore, in order to achieve stable energy levels, at least one of the nonlinear orders (i.e.  $\mu$  and  $\nu$ ) should be an odd number, for detailed discussion of the potential functions and how they are used to study the stability level of the system refer to [3].

Using this approach it is possible to compare the results for different configurations of  $\mu$  and  $\nu$ . Such systems with different parameters and orders of nonlinearities can be theoretically used for modelling some engineering applications. In principle, the symbolic computations method introduced in this work has the potential to be applied to general SDOF systems with any number of nonlinear terms. In order to test this method we start with two nonlinear terms described by Eq. (7) and increase the order, accordingly, it is possible to understand the capabilities and limitations of this method.

The following procedure illustrates the use of symbolic computations of a normal form method in order to solve Eq. (7) for  $\mu=2$  and  $\nu=7$ , nevertheless, following the same procedure, it is possible to solve the equation for any other values, as long as at least one exponent is odd.

Direct normal forms analysis of such systems undergoes a series of transformations that involve complex mathematical manipulations, in this work the most important results are shown, focusing on the utilization of symbolic computation software, i.e. Maple. Rewriting Eq. (7) with  $\mu=2$  and  $\nu=7$ , leads to

$$\ddot{x}(t) + \omega_n^2 x(t) + \alpha_1 x^2(t) + \alpha_2 x^7(t) = 0, \quad (8)$$

The first step is using Eq. (3) in view of Eq. (2) to make the linear modal transformation, in this step it should be noticed that for SDOF systems the transform is unity and  $x = q$ , then

$$\ddot{q} + \Lambda q + N_q(q) = 0, \text{ where } \Lambda = \omega_n^2 \text{ and } N_q(\mathbf{q}) = \alpha_1 q^2 + \alpha_2 q^7 \quad (9)$$

The second step is the near-identity transform, and for  $\varepsilon = 1$ , rewriting the nonlinear terms using  $\mathbf{u}$ , one should obtain  $N_q(u) = \alpha_1 u_1^2 + \alpha_2 u_1^7$  and  $\mathbf{u}_1 = \mathbf{u}_{p1} + \mathbf{u}_{m1}$ , thus

$$\mathbf{n}_{(1)}(\mathbf{u}) = \mathbf{n}^* \mathbf{u}^* (\mathbf{u}_p, \mathbf{u}_m) = \alpha_1 (u_{p1} + u_{m1})^2 + \alpha_2 (u_{p1} + u_{m1})^7 \quad (10)$$

Expanding Eq. (10),  $\mathbf{n}_{(1)}(\mathbf{u})$  will contain many terms (11 term in this case), these terms have to be primarily decomposed into coefficients and nonlinear functions vectors  $\mathbf{n}^*$  and  $\mathbf{u}^*$ , respectively.

$$\mathbf{n}^* = [\alpha_1 \quad \alpha_1 \quad \alpha_2 \quad \alpha_2 \quad 2\alpha_1 \quad 7\alpha_2 \quad 21\alpha_2 \quad 35\alpha_2 \quad 35\alpha_2 \quad 21\alpha_2 \quad 7\alpha_2] \quad (11a)$$

$$\mathbf{u}^* = [u_{m1}^2 \quad u_{p1}^2 \quad u_{m1}^7 \quad u_{p1}^7 \quad u_{p1}u_{m1} \quad u_{p1}u_{m1}^6 \quad u_{p1}^2u_{m1}^5 \quad u_{p1}^3u_{m1}^4 \quad u_{p1}^4u_{m1}^3 \quad u_{p1}^5u_{m1}^2 \quad u_{p1}^6u_{m1}]^T \quad (11b)$$

As the number of nonlinear terms and their corresponding orders increase, or when considering higher order accuracy (i.e.  $\varepsilon_2, \varepsilon_3, \dots$ ) this initial step becomes harder to be manipulated by usual hand calculations. Symbolically, the proposed algorithm can be efficiently completed to do this step and produce  $\mathbf{n}^*$  and  $\mathbf{u}^*$  matrices.

Using the proposed symbolic algorithm, we have been able to study several SDOF oscillators with two weak nonlinearities of variable orders. The key point in applying direct normal forms, especially for SDOF problems, is the number of terms involved in the matrices. Table 1 shows the number of terms for cases of conservative nonlinear oscillators of various orders of nonlinearities, i.e. for different configurations of  $\mu$  and  $\nu$ . Values in the highlighted cells represents the case when only one nonlinear term appears in the EOM.

Table (1): Number of terms involved in matrices for selected values of  $\nu$  and  $\mu$

| $\mu \backslash \nu$ | 3        | 5        | 7        | 9         | 11        | 13        |
|----------------------|----------|----------|----------|-----------|-----------|-----------|
| 2                    | 7        | 9        | 11       | 13        | 15        | 17        |
| 3                    | <b>4</b> | 10       | 12       | 14        | 16        | 18        |
| 4                    | 9        | 11       | 13       | 15        | 17        | 19        |
| 5                    | 10       | <b>6</b> | 14       | 16        | 18        | 20        |
| 6                    | 11       | 13       | 15       | 17        | 19        | 21        |
| 7                    | 12       | 14       | <b>8</b> | 18        | 20        | 22        |
| 8                    | 13       | 15       | 17       | 19        | 21        | 23        |
| 9                    | 14       | 16       | 18       | <b>10</b> | 22        | 24        |
| 10                   | 15       | 17       | 19       | 21        | 23        | 25        |
| 11                   | 16       | 18       | 20       | 22        | <b>12</b> | 26        |
| 12                   | 17       | 19       | 21       | 23        | 25        | 27        |
| 13                   | 18       | 20       | 22       | 24        | 25        | <b>14</b> |



The increasing number of terms appearing in Table 1 leads to additional difficulties for hand calculations to be performed. Importantly, more complex systems will lead to a higher number of terms; some examples of more complex cases include:

- the EOM involves viscous damping (in this case two additional terms are to be added to those in Table 1),
- the system contains more than two types of polynomial nonlinearities,
- solving the EOM for a higher order accuracy (i.e.  $\varepsilon_2$ )
- and when using the direct normal forms technique for MDOF systems,

all of the aforementioned cases can yield to a dramatic increase in the size of the matrices, thus, the mathematical complexity is also increased, these causes can justify turning to symbolic computation method.

In order to complete the analysis, by applying Eq. (6),  $\boldsymbol{\beta}^*$  can be written as

$$\boldsymbol{\beta}^* = \begin{bmatrix} 3\omega_{r1}^2 & 48\omega_{r1}^2 & 3\omega_{r1}^2 & 48\omega_{r1}^2 & -\omega_{r1}^2 & 24\omega_{r1}^2 & 8\omega_{r1}^2 & 0 & 0 & 8\omega_{r1}^2 & 24\omega_{r1}^2 \end{bmatrix} \quad (12)$$

It should be emphasized that, according to direct normal forms analysis, any *zero* value in  $\boldsymbol{\beta}^*$  matrix indicates the presence of a resonant term; while any *nonzero* value indicates a non-resonant or harmonic term.

The next step, illustrates the resulting coefficients of resonant terms  $\mathbf{n}_u^*$  and of harmonic terms  $\mathbf{h}^*$  for both resonant and non-resonant cases (refer to [3] for detailed analysis). In symbolic programming, this step is based on conditional loop manipulation for each element in  $\boldsymbol{\beta}^*$  with respect to  $\mathbf{n}^*$ . The results are

$$\mathbf{n}_u^* = \alpha_2 [0 \ 0 \ 0 \ 0 \ 0 \ 0 \ 0 \ 35 \ 35 \ 0 \ 0] \quad (13a)$$

$$\mathbf{h}^* = \frac{1}{\omega_{r1}^2} \begin{bmatrix} \alpha_1 & \alpha_1 & \alpha_2 & \alpha_2 & -2\alpha_1 & \frac{7\alpha_2}{24} & \frac{21\alpha_2}{8} & 0 & 0 & \frac{21\alpha_2}{8} & \frac{7\alpha_2}{24} \end{bmatrix} \quad (13b)$$

If the analysis is only truncated to  $\varepsilon_1$  accuracy, which regularly leads to acceptable inspection of the nonlinear effects of small nonlinearities, the final step is rewriting the transformed equation of motion. For the non-resonant case, Eq. (9) in  $u$ -transformed coordinate system becomes

$$\ddot{\mathbf{u}} + \mathcal{A}\mathbf{u} + \mathbf{n}_u^* \mathbf{u}^* = 0,$$

$$\ddot{\mathbf{u}} + \omega_n^2 \mathbf{u} + 35 \left( u_{p1}^3 u_{m1}^4 + u_{p1}^4 u_{m1}^3 \right) = 0, \quad (14)$$

and the near identity transform is written as

$$\mathbf{q} = \mathbf{u} + \mathbf{h}^* \mathbf{u}^*,$$

$$\mathbf{q} = \mathbf{u} + \frac{1}{3\omega_{r1}^2} \left( \begin{array}{l} \alpha_1 u_{m1}^2 + \frac{\alpha_1 u_{p1}^2}{16} + \alpha_2 u_{m1}^7 + \frac{\alpha_2 u_{p1}^7}{16} - 6\alpha_1 u_{p1} u_{m1} + \frac{7\alpha_2 u_{p1} u_{m1}^6}{8} + \\ \frac{63\alpha_2 u_{p1}^2 u_{m1}^5}{8} + \frac{63\alpha_2 u_{p1}^5 u_{m1}^2}{8} + \frac{7\alpha_2 u_{p1}^6 u_{m1}}{8} \end{array} \right) \quad (15)$$

Substituting in the assumed solution Eq. (4), and solving the positive (or negative) complex exponential terms by exact balancing, one can get the equation of the backbone curve for this system, which is

$$\omega_{r1}^2 = \omega_n^2 + \frac{35}{64} \alpha_2 U^6 \quad (16)$$

Following the same aforementioned procedure, one should be able of finding the backbone curve for any values of  $\nu$  and  $\mu$  in Eq. (7). One advantage of having a computer pattern in such case is the ability of doing several runs with different conditions. Table 2 shows the backbone curve obtained for the first four values of  $\nu$  when  $\mu = 2$  for the  $\varepsilon_1$  expansion. It is clear that a general pattern is repeated for the backbone equation found, so if  $\mu = 2$  it could be generalized for any value of  $\nu$  that

$$\omega_{r1}^2 = \omega_n^2 + \eta_i \alpha_2 U^{\nu-1}, \quad \nu = 3, 5, 7, \dots \quad (17)$$

Where  $\eta_i$  is a constant.

Table (2): Backbone curve equations of  $\varepsilon_1$  accuracy for different values of  $\nu$  while  $\mu = 2$

| Value of $\nu$ | Equation of motion  | Backbone curve equation                                    |
|----------------|---|--|
| 3              | $\ddot{x}(t) + \omega_n^2 x(t) + \alpha_1 x^2(t) + \alpha_2 x^3(t) = 0$ | $\omega_{r1}^2 = \omega_n^2 + \frac{3}{4} \alpha_2 U^2$    |
| 5              | $\ddot{x}(t) + \omega_n^2 x(t) + \alpha_1 x^2(t) + \alpha_2 x^5(t) = 0$ | $\omega_{r1}^2 = \omega_n^2 + \frac{5}{8} \alpha_2 U^4$    |
| 7              | $\ddot{x}(t) + \omega_n^2 x(t) + \alpha_1 x^2(t) + \alpha_2 x^7(t) = 0$ | $\omega_{r1}^2 = \omega_n^2 + \frac{35}{64} \alpha_2 U^6$  |
| 9              | $\ddot{x}(t) + \omega_n^2 x(t) + \alpha_1 x^2(t) + \alpha_2 x^9(t) = 0$ | $\omega_{r1}^2 = \omega_n^2 + \frac{63}{128} \alpha_2 U^8$ |

Practically, for weak nonlinear case, the values of  $\alpha_1$  and  $\alpha_2$  should be small, typically less than unity, Fig. (1) shows the backbone curves for the conservative oscillators appearing in Table 2, using the following numerical values;  $\alpha_1 = 0.2$ ,  $\alpha_2 = 0.1$  and  $\omega_n = \pi$  rad/s.

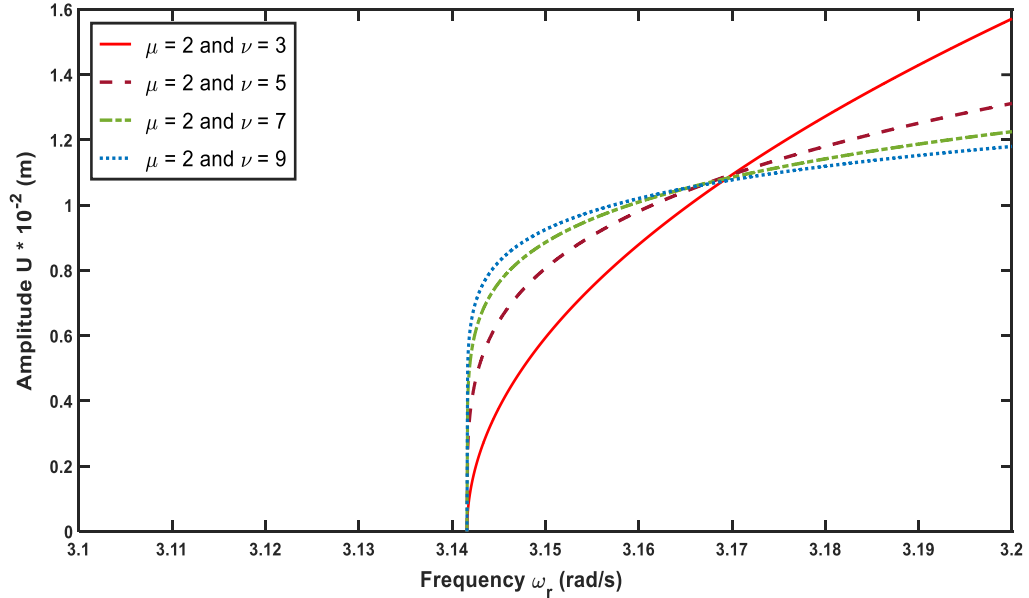


Fig. (1): Conservative backbone curves for different values of  $\nu$  while  $\mu = 2$

Furthermore, we could obtain the backbone curve relation truncated to  $\varepsilon_1$  accuracy for any values of  $\nu$  and  $\mu$  in Eq. (7). Table 3 shows some examples of these results.

Table (3): Backbone curve equations of  $\varepsilon_1$  accuracy for different values of  $\nu$  and  $\mu$

| Value of $\nu$ | Value of $\mu$ | Equation of motion   | Backbone curve equation   |
|----------------|----------------|--|---|
| 3              | 5              | $\ddot{x}(t) + \omega_n^2 x(t) + \alpha_1 x^3(t) + \alpha_2 x^5(t) = 0$    | $\omega_{r1}^2 = \omega_n^2 + \frac{3}{4} \alpha_1 U^2 + \frac{5}{8} \alpha_2 U^4$          |
| 4              | 7              | $\ddot{x}(t) + \omega_n^2 x(t) + \alpha_1 x^4(t) + \alpha_2 x^7(t) = 0$    | $\omega_{r1}^2 = \omega_n^2 + \frac{35}{64} \alpha_2 U^6$                                   |
| 5              | 9              | $\ddot{x}(t) + \omega_n^2 x(t) + \alpha_1 x^5(t) + \alpha_2 x^9(t) = 0$    | $\omega_{r1}^2 = \omega_n^2 + \frac{5}{8} \alpha_1 U^4 + \frac{63}{128} \alpha_2 U^8$       |
| 6              | 9              | $\ddot{x}(t) + \omega_n^2 x(t) + \alpha_1 x^6(t) + \alpha_2 x^9(t) = 0$    | $\omega_{r1}^2 = \omega_n^2 + \frac{63}{128} \alpha_2 U^8$                                  |
| 7              | 11             | $\ddot{x}(t) + \omega_n^2 x(t) + \alpha_1 x^7(t) + \alpha_2 x^{11}(t) = 0$ | $\omega_{r1}^2 = \omega_n^2 + \frac{35}{64} \alpha_2 U^6 + \frac{231}{512} \alpha_2 U^{10}$ |

The following findings are noted:

- Any even nonlinearity found in the EOM is removed by the normal form transformation and does not appear in the backbone curve. This phenomenon is found in literature in terms of quadratic nonlinearity, here we generalise this finding for any even nonlinearity.
- Referring to Table 3 and comparing with Table 2, it is clear that the frequency detuning accompanied with direct normal forms resulted in, at least for  $\varepsilon_1$  accuracy, a behavior similar to superposition regarding the final backbone curve expression.
- Some of these results are numerically verified using COCO numerical continuation toolbox in Matlab (see Fig. (3)), and acceptable agreement between analytical backbone curves and numerical backbone manifolds is seen.

In conclusion, in order to generalise the  $\varepsilon_1$  backbone curve relation for any SDOF nonlinear oscillator with two types of nonlinearities, Eq. (7), in view of Table 1 and Table 2, provided that  $\nu$  and  $\mu$  are odd, the following relation can be obtained

$$\omega_{r1}^2 = \omega_n^2 + \eta_1 \alpha_1 U^{\nu-1} + \eta_2 \alpha_2 U^{\mu-1} \quad (18)$$

Where  $\eta_1$  and  $\eta_2$  are constants directly related to the order of the nonlinearity, Table 4 shows the values of this constant for several orders of the nonlinear terms. Finally, as mentioned earlier, any even nonlinearity in the EOM will be removed by the normal form and will not appear in Eq. (18).

Table (4): Values of the constant  $\eta_i$  appearing in the backbone curve relation, Eq. (18)

| Order of nonlinearity | 3             | 5             | 7               | 9                | 11                | 13                 | 15                   | 17                    |
|-----------------------|---------------|---------------|-----------------|------------------|-------------------|--------------------|----------------------|-----------------------|
| $\eta_i$              | $\frac{3}{4}$ | $\frac{5}{8}$ | $\frac{35}{64}$ | $\frac{63}{128}$ | $\frac{231}{512}$ | $\frac{429}{1024}$ | $\frac{6435}{16384}$ | $\frac{12155}{32768}$ |

Using Eq. (18) and Table 4 it is possible to get the conservative backbone curve relation for any nonlinear oscillator with two different types of polynomial nonlinearities. As an example, if the EOM contains both cubic and quintic nonlinearities, i.e.

$$\ddot{x}(t) + \omega_n^2 x(t) + \alpha_1 x^3(t) + \alpha_2 x^5(t) = 0,$$

then, the conservative backbone curve of  $\varepsilon_1$  accuracy will be

$$\omega_{r1}^2 = \omega_n^2 + \frac{3}{4} \alpha_1 U^2 + \frac{5}{8} \alpha_2 U^4$$

### 2.3 Non-resonant Duffing oscillator with cubic nonlinearity

As an example of a more complex system, we now consider the system of a Duffing oscillator with cubic nonlinearity, viscous damping and forcing away from resonance where the ratio between the driving frequency and the natural frequency is  $1/3$  (i.e.  $a = 1/3$ ),

$$\ddot{x}(t) + 2\zeta\omega_n\dot{x}(t) + \omega_n^2x(t) + \alpha x^3(t) = R \cos(\Omega t) \quad (19)$$

Using the proposed direct normal forms technique applied symbolically, it is required to generate analytical conservative backbone curve equations for  $\varepsilon_1$  accuracy, and compare with forced (and lightly damped) response curves. The step by step procedure involves large matrices and algebraic terms, hence, only the key results are to be shown, while further results for matrix algebra manipulations can be found in Appendix 1. After applying direct normal forms analysis we get

$$\frac{1}{4} \left[ 3\alpha U_1^3 + (24\alpha e^2 + 4(\omega_n^2 - \omega_{r1}^2)) \right] \cos(\omega_{r1}t - \phi_1) + 2\alpha e^3 \cos(\omega_{r1}t) - 2\zeta\omega_n\omega_{r1}U_1 \sin(\omega_{r1}t - \phi_1) = 0 \quad (20)$$

Where  $e = \frac{R}{2(\omega_n^2 - \Omega^2)}$ .

Applying the suitable trigonometric identities, and then balancing the sines and cosines terms in Eq. (20) we get

$$\zeta\omega_n\omega_{r1}U = -\alpha e^3 \sin(\phi_1) \quad (21a)$$

$$3\alpha e^2 + \frac{3}{8}\alpha U_1^3 + \frac{1}{2}(\omega_n^2 - \omega_{r1}^2) = -\alpha e^3 \cos(\phi_1) \quad (21b)$$

Hence, it is possible to use Eq. (21) to get an expression for  $U$  as a function of  $\omega_{r1}$ , therefore, computing the forced response curve analytically, this has been previously done in [3] by applying traditional hand calculations. In order to compare with our proposed symbolic computation method, the same problem has been solved in conservative case (unforced-undamped case), and the conservative backbone curve is computed using Eq. (18) and Table (4) and plotted in Fig. (2), along with the analytically computed forced-damped response curves for several values of  $R$  using Eq. (21). The numerical values chosen for this figure are  $\omega_n = 2$  rad/s,  $\zeta = 0.01$  and  $\alpha = 0.2$ .

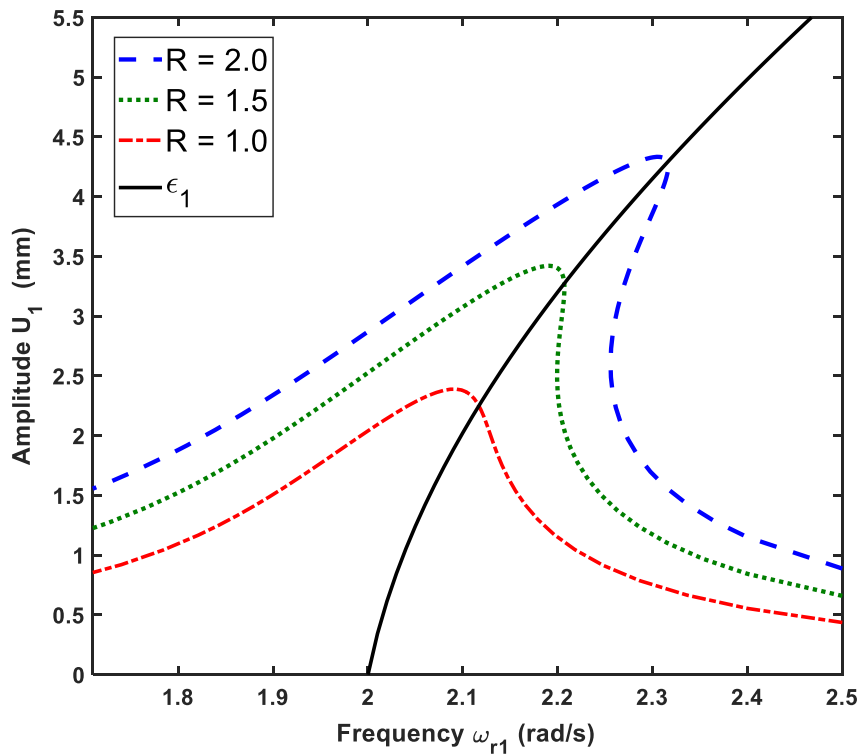


Fig. (2): Backbone curve of damped forced Duffing oscillator with cubic nonlinearity

Figure (2) represents a typical backbone curve and response curves for any forced damped nonlinear system. From this figure, several important observations can be noticed; first of all, as the value of  $\alpha$  is positive, hardening behavior is clearly seen, in contrary, if  $\alpha$  is negative softening behavior will be noticed. Furthermore, as the figure shows the relation between natural frequency and amplitude, the backbone curves do not perfectly coincide with the manifolds, and this is due to the presence of damping. Finally, as the forcing amplitude  $R$  becomes higher, more matching between the backbone curves and their manifolds occurs.

Finally, in order to compare the frequency response of several nonlinear terms in combination, recall Eq. (5) in its forced damped case, that is

$$\ddot{x}(t) + 2\zeta\omega_n\dot{x}(t) + \omega_n^2x(t) + \alpha_1x^\nu(t) + \alpha_2x^\mu(t) = R\cos(\Omega t) \quad (22)$$

Various values of  $\nu$  and  $\mu$  can be considered, the corresponding EOM can be studied using direct normal forms and analytical backbone curve relations are then obtained. Three cases are studied, linear oscillator and cubic-quintic oscillator in both hardening and softening cases (3-5 Hardening, 3-5 Softening). Figure 3 represents backbone equation for all previous cases along with their forcing manifolds obtained numerically using COCO. Figure 3 is generated using the numerical data: general parameters for all cases  $\omega_n = 2$  Hz,  $\zeta = 0.05$  and  $R = 1$ . In the case of hardening cubic-quintic oscillator  $\alpha_1 = 0.2$  and  $\alpha_2 = 0.3$ . Finally, for softening cubic-quintic oscillator  $\alpha_1 = -0.2$  and  $\alpha_2 = -0.3$ .

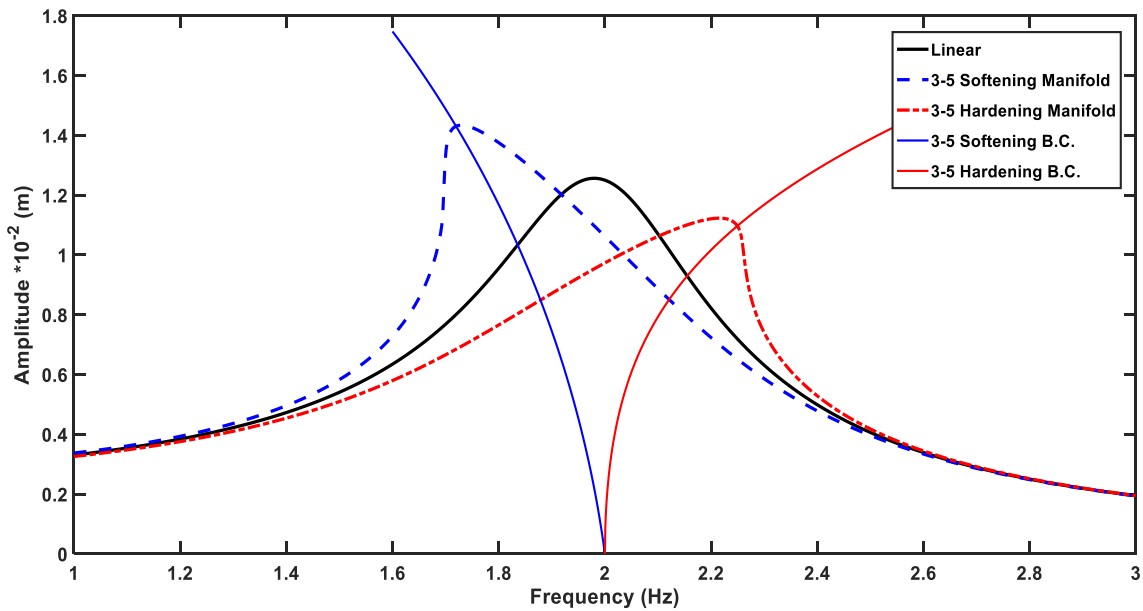


Fig. (3): Frequency response of various types of nonlinearities

Figure 3 illustrates the effect of both hardening and softening nonlinear terms on the frequency response of the system; firstly, compared to the linear case, hardening polynomial nonlinearities shift the peak to the right whilst minimizing the maximum vibration amplitude of the system. On the other hand, softening nonlinear terms cause shifting to the left and maximizing the vibration amplitude. However, using Eq. (18) along with Table 4 it is possible to obtain the conservative backbone curves for SDOF oscillator with two nonlinear terms, and compare with the forced-damped frequency response computed numerically using COCO toolbox in Matlab.

### 3 CONCLUSION

In this work, the direct normal forms method is used to study the dynamical behavior of SDOF oscillators with higher orders of polynomial nonlinearities. Symbolic computations using Maple were implemented for the analytical solutions, where backbone curves expressions of  $\varepsilon_1$  order were obtained and the results were verified using COCO numerical continuation toolbox in Matlab. A general formula for any SDOF nonlinear oscillator with two polynomial nonlinearities are obtained by computing high number of terms in the solution (refer to Table 1).

The overall truncated analytical results show good agreement with the numerical results, accordingly, extending the direct normal forms using symbolic computations can yield to some desired findings regarding the dynamics of the system. Although the proposed technique overcomes the mathematical complexities and enables fast analysis of SDOF nonlinear oscillators, its limited to weakly nonlinear systems where the nonlinear terms are modelled by polynomial terms in the EOM, so that the direct normal forms technique is applicable.

Overall, the work shows good insight regarding the implementation of symbolic computations when studying SDOF nonlinear oscillators, where we have been able to analytically compute the conservative backbone curves for any SDOF oscillator with two nonlinear terms.

## ACKNOWLEDGEMENTS

Ayman M. Nasir has a scholarship funded by Alzaytoonah University of Jordan in order to obtain his PhD degree.

## REFERENCES

- [1] Jack K Hale. Oscillations in nonlinear systems. *McGraw-Hill*, 1963.
- [2] Minoru Urabe. Nonlinear autonomous oscillations: Analytical theory, volume 34. *Academic Press*, 1967.
- [3] Wagg D, Neild S. A., Nonlinear vibration with control: for flexible and adaptive structures. *Solid Mechanics and its Applications*, 2nd edition, vol. 218. Berlin, Germany: Springer, 2014.
- [4] Nayfeh A., Mook D. Nonlinear oscillations. *New York, NY: Wiley*, 1995.
- [5] Everett Minnich Baily. Steady-state harmonic analysis of nonlinear networks. PhD thesis, Department of Electrical Engineering, *Stanford University*, 1968.
- [6] JOHN C Lindenlaub, An approach for finding the sinusoidal steady state response of nonlinear systems. In Proc. 7th Ann. Allerton Conf. Circuit and System Theory. Univ. Illinois, 1969.
- [7] S. Wang and K. Huseyin. ‘Maple’ Analysis of nonlinear oscillations, *Mathematical and Computer Modelling*, Vol. 16, No. 11, pp. 49-57, 1992.
- [8] Z.F. Xin, S.A. Neild, D.J. Wagg, and Z.X. Zuo. Resonant response functions for nonlinear oscillators with polynomial type nonlinearities. *Journal of Sound and Vibration*, 332 (7): 1777–1788, 2013.
- [9] T. L. Hill, A. Cammarano, SA Neild, and DJ Wagg. An analytical method for the optimisation of weakly nonlinear systems. *Proceedings of EURO DYN 2014*, pages 1981–1988, 2014.
- [10] A. H. Nayfeh, Perturbation Methods, *Wiley, New York*, 1973.
- [11] F. Schilder and H. Dankowicz. Recipes for Continuation, *SIAM Computational Science and Engineering*, 2013.
- [12] F. Schilder and H. Dankowicz. Continuation core and toolboxes (coco). Available at <https://sourceforge.net/projects/cocotools/>, 2017.
- [13] J. Thomsen, Vibrations and Stability: Order and Chaos, *McGraw Hill*, 1997.
- [14] D. Richards, Advanced mathematical methods with Maple, *Cambridge University Press*, 2009.



- [15] R. Enns and G. McGuire, *Nonlinear physics with Maple for scientists and engineers*, Springer, 2000.
- [16] S. Bellizzi and R. Bouc. A new formulation for the existence and calculation for nonlinear normal modes. *Journal of Sound and Vibration*, 287(3): 545-569, (2005).
- [17] X. Lui, *Symbolic Tools for the Analysis of nonlinear dynamical systems*, PhD thesis, Department of Applied Mathematics, *University of Western Ontario*, London, 1999.
- [18] Liu, X., & Wagg, D. J.  $\varepsilon_2$ - order normal form analysis for a two-degree-of-freedom nonlinear coupled oscillator. *Submitted to appear in Proceedings of the First International Nonlinear Dynamics Conference (2019)*.
- [19] P. B. Kahn and Y. Zarmi, *Nonlinear dynamics: Exploration through normal forms*, Dover Publications, New York, USA, 2014
- [20] T. Breunung and G. Haller, Explicit backbone curves from spectral submanifolds of forced-damped nonlinear mechanical systems. *Proc. R. Soc. A* 474, 20180083, 2018.
- [21] Kenneth Meyer, Glen Hall, and Dan Offin, *Introduction to Hamiltonian dynamical systems and the n-body problem: A Mechanised Logic of Computation*, volume 90. *Springer Science & Business Media*, 2008.
- [22] Vladimir Igorevich Arnold, *Geometrical methods in the theory of ordinary differential equations*, volume 250. *Springer Science & Business Media*, 2012.
- [23] A. D. Shaw, S. A. Neild, and D. J. Wagg. Dynamic analysis of high static low dynamic stiffness vibration isolation mounts. *Journal of Sound and Vibration*, 332:1437–1455, 2012.
- [24] Jezequel, L. and Lamarque, C. H. Analysis of nonlinear dynamic systems by the normal form theory. *Journal of Sound and Vibration*, 149(3), 429–459, 1991.
- [25] A. H. Nayfeh, *Method of normal forms*, Wiley, New York, 1993.

## APPENDIX 1

**Matrix manipulation of forced damped Duffing oscillator of cubic order nonlinearity, with forcing away from resonance.**

$$\mathbf{u}^* = \begin{bmatrix} r_m^3 \\ r_p^3 \\ u_{m1}^3 \\ u_p^3 \\ r_p r_m^2 \\ r_m r_p^2 \\ u_m r_m^2 \\ u_m r_p^2 \\ r_m u_m^2 \\ r_p u_m^2 \\ u_p r_m^2 \\ u_p r_p^2 \\ u_p u_m^2 \\ r_m u_p^2 \\ r_p u_p^2 \\ u_m u_p^2 \\ u_m r_m r_p \\ u_p r_m r_p \\ u_p u_m r_m \\ u_p u_m r_p \\ r_m \\ r_p \\ u_m \\ u_p^2 \end{bmatrix} \rightarrow (\boldsymbol{\beta}^*)^T = \omega_{r1}^2 \begin{bmatrix} 0 \\ a^2 - 1 \\ 0 \\ a^2 - 1 \\ 0 \\ a^2 - 1 \\ a^2 - 1 \\ 0 \\ 8 \\ 8 \\ 0 \\ 9a^2 - 1 \\ 9a^2 - 1 \\ a^2 - 4a + 3 \\ a^2 - 4a + 3 \\ 4a(a-1) \\ 4a(a+1) \\ a^2 - 1 \\ 4a(a-1) \\ a^2 + 4a + 3 \\ 4a(a+1) \\ a^2 + 4a + 3 \\ a^2 - 1 \end{bmatrix} \xrightarrow{\text{Substitute } a=1/3} (\boldsymbol{\beta}^*)^T = \omega_{r1}^2 \begin{bmatrix} 0 \\ \frac{8}{9} \\ 0 \\ -\frac{8}{9} \\ -\frac{8}{9} \\ 0 \\ 8 \\ 8 \\ 0 \\ 0 \\ 0 \\ \frac{16}{9} \\ \frac{16}{9} \\ -\frac{8}{9} \\ \frac{16}{9} \\ -\frac{8}{9} \\ \frac{16}{9} \\ -\frac{8}{9} \\ -\frac{8}{9} \\ \frac{40}{9} \\ \frac{16}{9} \\ \frac{16}{9} \\ -\frac{8}{9} \end{bmatrix} \rightarrow \mathbf{h}^* = \frac{1}{\omega_{r1}^2} \begin{bmatrix} 0 \\ \frac{9}{12} i e \zeta \omega_n \\ 0 \\ -\frac{9}{12} i e \zeta \omega_n \\ 0 \\ -\frac{27}{4} \alpha e \\ -\frac{27}{4} \alpha e \\ 0 \\ \frac{\alpha}{8} \\ \frac{\alpha}{8} \\ 0 \\ \frac{27}{16} \alpha e \\ \frac{16}{27} \alpha e \\ \frac{16}{27} \alpha e \\ -\frac{27}{8} \alpha e^2 \\ \frac{27}{16} \alpha e^2 \\ -\frac{27}{16} \alpha e^2 \\ -\frac{27}{8} \alpha e^3 \\ -\frac{27}{8} \alpha e^2 \\ \frac{8}{27} \alpha e \\ \frac{40}{27} \alpha e^2 \\ \frac{16}{27} \alpha e \\ \frac{40}{27} \alpha e \\ -\frac{27}{8} \alpha e^3 \end{bmatrix}$$